

See discussions, stats, and author profiles for this publication at: <https://www.researchgate.net/publication/224808252>

Mercury Distribution and Deposition in Glacier Snow over Western China

ARTICLE in ENVIRONMENTAL SCIENCE & TECHNOLOGY · APRIL 2012

Impact Factor: 5.33 · DOI: 10.1021/es300166x · Source: PubMed

CITATIONS

22

READS

53

9 AUTHORS, INCLUDING:



Mark Loewen

University of Manitoba

14 PUBLICATIONS 285 CITATIONS

SEE PROFILE



Jianzhong Xu

Chinese Academy of Sciences

24 PUBLICATIONS 285 CITATIONS

SEE PROFILE



Yulan Zhang

Chinese Academy of Sciences

20 PUBLICATIONS 173 CITATIONS

SEE PROFILE



Shichang Kang

Chinese Academy of Sciences

367 PUBLICATIONS 4,961 CITATIONS

SEE PROFILE

Mercury Distribution and Deposition in Glacier Snow over Western China

Qianggong Zhang,[†] Jie Huang,[†] Feiyue Wang,^{‡,§} Loewen Mark,[‡] Jianzhong Xu,[§] Debbie Armstrong,[‡] Chaoliu Li,[†] Yulan Zhang,[†] and Shichang Kang^{*,†,§}

[†]Key Laboratory of Tibetan Environment Changes and Land Surface Processes, Institute of Tibetan Plateau Research, Chinese Academy of Sciences, Jia 4 Datun Road, Chaoyang District, Beijing, 100101, P.R. China

[‡]Department of Chemistry, and [§]Department of Environment and Geography, University of Manitoba, Winnipeg, MB R3T 2N2, Canada

[§]State Key Laboratory of Cryospheric Sciences, Cold and Arid Regions Environmental and Engineering Research Institute, Chinese Academy of Sciences, Lanzhou, 730000, P.R. China

S Supporting Information

ABSTRACT: Western China is home to the largest aggregate of glaciers outside the polar regions, yet little is known about how the glaciers in this area affect the transport and cycling of mercury (Hg) regionally and globally. From 2005 to 2010, extensive glacier snow sampling campaigns were carried out in 14 snowpits from 9 glaciers over western China, and the vertical distribution profiles of Hg were obtained. The Total Hg (THg) concentrations in the glacier snow ranged from <1 to 43.6 ng L⁻¹, and exhibited clear seasonal variations with lower values in summer than in winter. Spatially, higher THg concentrations were typically observed in glacier snows from the northern region where atmospheric particulate loading is comparably high. Glacier snowpit Hg was largely dependent on particulate matters and was associated with particulate Hg, which is less prone to postdepositional changes, thus providing a valuable record of atmospheric Hg deposition. Estimated atmospheric Hg depositional fluxes ranged from 0.74 to 7.89 $\mu\text{g m}^{-2} \text{yr}^{-1}$, agreeing very well with the global natural values, but are one to two orders of magnitude lower than that of the neighboring East Asia. Elevated Hg concentrations were observed in refrozen ice layers in several snowpits subjected to intense melt, indicating that Hg can be potentially released to meltwater.



INTRODUCTION

Mercury (Hg) is ubiquitous in the environment and has been recognized as a global contaminant due to its long-range transport via the atmosphere, biomagnification in ecosystems, and its intrinsic toxicity.¹ Hg is involved in numerous complex environmental processes and its atmospheric, aquatic, and biological cycles have been a subject of significant scientific interest over the past decades.² As a transitional medium between the atmosphere and aquatic ecosystems, snow and ice have been shown to play a pivotal role in Hg cycling in polar regions (e.g., refs 2 and 3 and literatures therein). However, much less is known about Hg behavior in alpine regions in mid- and low-latitude areas. This represents a major knowledge gap, as many mid- and low-latitude alpine regions are in close

vicinity to high human population densities. Consequently, Hg cycles in these regions are more susceptible to the impact of human activities and potentially pose health risk to a large number of human population.

Western China, defined herein as the Tibetan Plateau and the Xinjiang Uyghur Autonomous Region of China, is the most glacier concentrated region at low- and mid-latitudes.⁴ The region is also the source of water for more than one-third of the world's population.⁵ By examining Hg profiles in snowpits from

Received: January 14, 2012

Revised: April 11, 2012

Accepted: April 22, 2012

Published: April 22, 2012

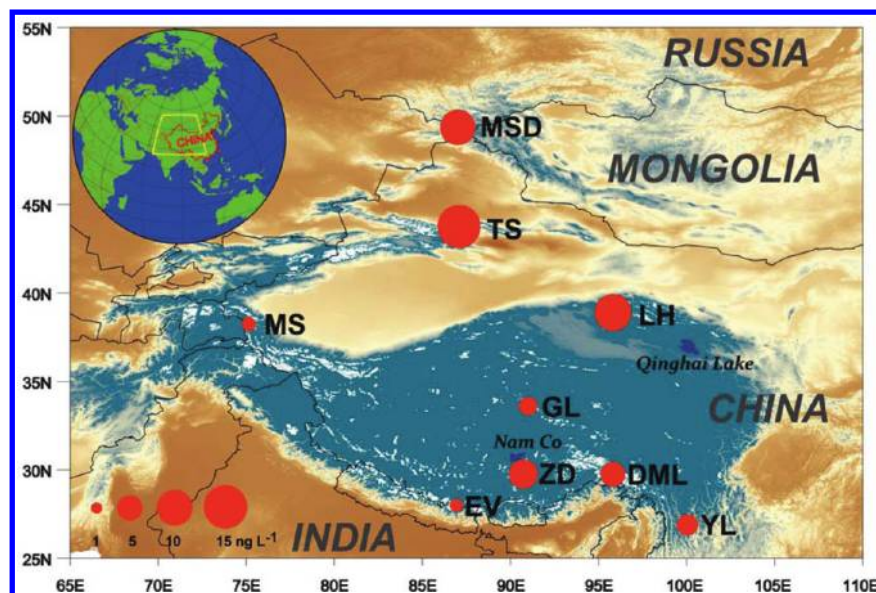


Figure 1. Map showing the snowpit sampling sites on glaciers in western China. The red circle shows the location of the sampling site, while its area represents the average THg concentration from the site.

3 glaciers in the central Tibetan Plateau, we recently reported a strong seasonal signal in Hg deposition in the region.⁶ Similar seasonal variations were also reported based on Hg time series reconstructed from a shallow firn core drilled at the Dasuopu Glacier in the central Himalaya.⁷ These studies suggest that snowpits and ice cores in low- and mid-latitude glaciers could be potentially used to study the past atmospheric Hg changes at seasonal or annual scales.

Building upon these studies, we performed extensive sampling campaigns from 2005 to 2010 and obtained snow samples from 14 snowpits over the vast region of western China. Total mercury (THg) and other parameters including stable oxygen isotope, major ions and insoluble particles were measured to conduct a thorough assessment of spatial-temporal variability of Hg over this region. These campaigns represent the most extensive snowpit Hg sampling in central Asia and perhaps the entire low- to mid-latitude regions. The results allowed us to evaluate not only the spatiotemporal variations in THg in glacier snowpits but also the possibility of using THg records in glacier snowpits as a practical tool for estimating atmospheric Hg depositional fluxes in remote and harsh environments.

MATERIALS AND METHODS

Sampling Sites. Western China is characterized by the world's highest and largest plateau (Tibetan Plateau) in the south and vast deserts in the north. On top of the world's highest mountain ranges and peaks is the largest aggregate of glaciers outside the polar regions. It is climatically complex, influenced to various degrees by the Indian monsoon, westerly jet stream, polar continental air masses, and East Asia summer monsoon (Supporting Information). A total of 14 snowpits were sampled from 9 glaciers (Figure 1 and Table S1 of the Supporting Information) including the Musidao glacier (MSD), the Tianshan Urumqi No.1 glacier (TS), the Laohugou No.12 glacier (LH), the Muztag glacier (MS), the Geladiandong Guoqu glacier (GL), the Zhadang glacier (ZD), the Demula glacier (DML), the Mount Everest East Rongbuk glacier (EV), and the Mount Yulong Baishui No. 1 glacier (YL). The

sampling altitudes ranged from 3605 m at MSD to 6536 m at EV. The sampling was carried out from May 2005 to August 2010, with several sites (GL, ZD and EV) being sampled in multiple years (Table S1 of the Supporting Information).

Snowpit Sampling. At each sampling site, a snowpit was dug into the snowpack with a depth around 1–2 m. Snow samples were collected from the snowpit with a vertical resolution of 5–20 cm (Table S1 of the Supporting Information) following the “Clean Hands-Dirty Hands” protocol as described in our previous work.⁶ Briefly, all snow samples were stored in precleaned 500-mL amber glass jars with Teflon liners or in 50 mL new polypropylene Falcon tubes and were immediately doubly packed in Ziploc bags; the Falcon tubes and amber glass jars were randomly tested for background Hg levels and were always below the detection limit of 0.2 ng L⁻¹. Ultraclean HCl (250 μ L CMOS grade from J.T. Baker for 500-mL glass jars, or 100 μ L BV–III grade from Beihua Chemical, China for 50-mL tubes) was spiked to the samples on site or in clean rooms within 24 h after the sampling where field conditions precluded the onsite spike. Snow samples for other parameters such as $\delta^{18}\text{O}$, major ions, and insoluble particles were collected at the same time and were stored in Whirl-Pak bags kept frozen in a dark freezer. They were melted at room temperature in a clean room and then were split into small HDPE vials.

A 60 cm shallow snowpit was dug in September 2010 at site ZD to quantify particulate-bound Hg (PHg). Two samples were collected in each snow layer, the one for THg determination was treated as described previously; the other for dissolved mercury (DHg) analysis was melted at room temperature and filtered through a 0.45 μ m membrane (Durapore, Millipore), then was acidified to 0.5% (v/v) with HCL for preservation. PHg was estimated by the difference between THg and DHg. All the samples were stored at 4 $^{\circ}\text{C}$ until analysis.

Sample Analysis. THg concentration was quantified by cold vapor atomic fluorescence spectrometry following U.S.EPA Method 1631⁸ using a Tekran 2600 at the Ultra-Clean Trace Elements Laboratory (UCTEL) at the University

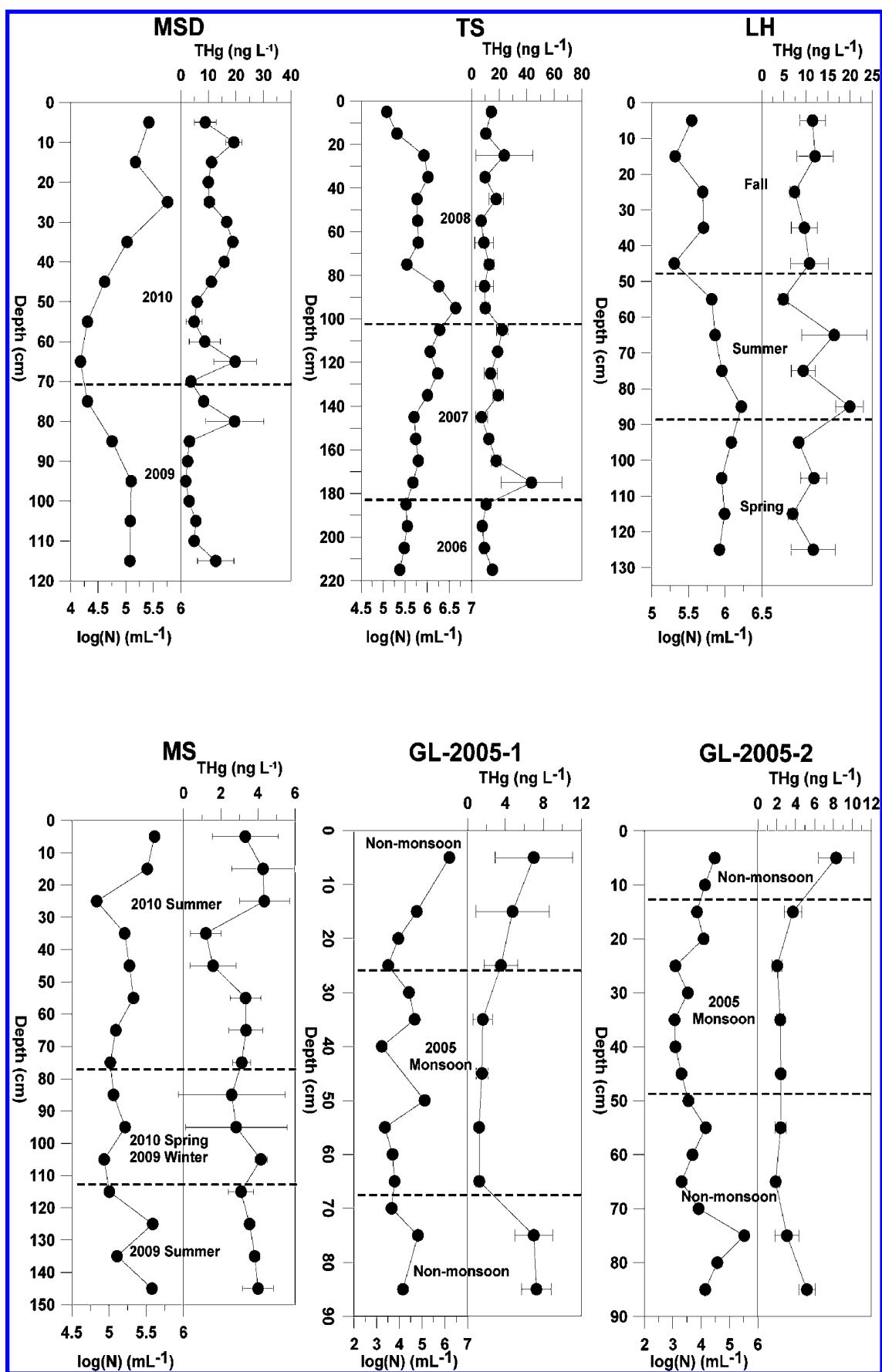


Figure 2. continued

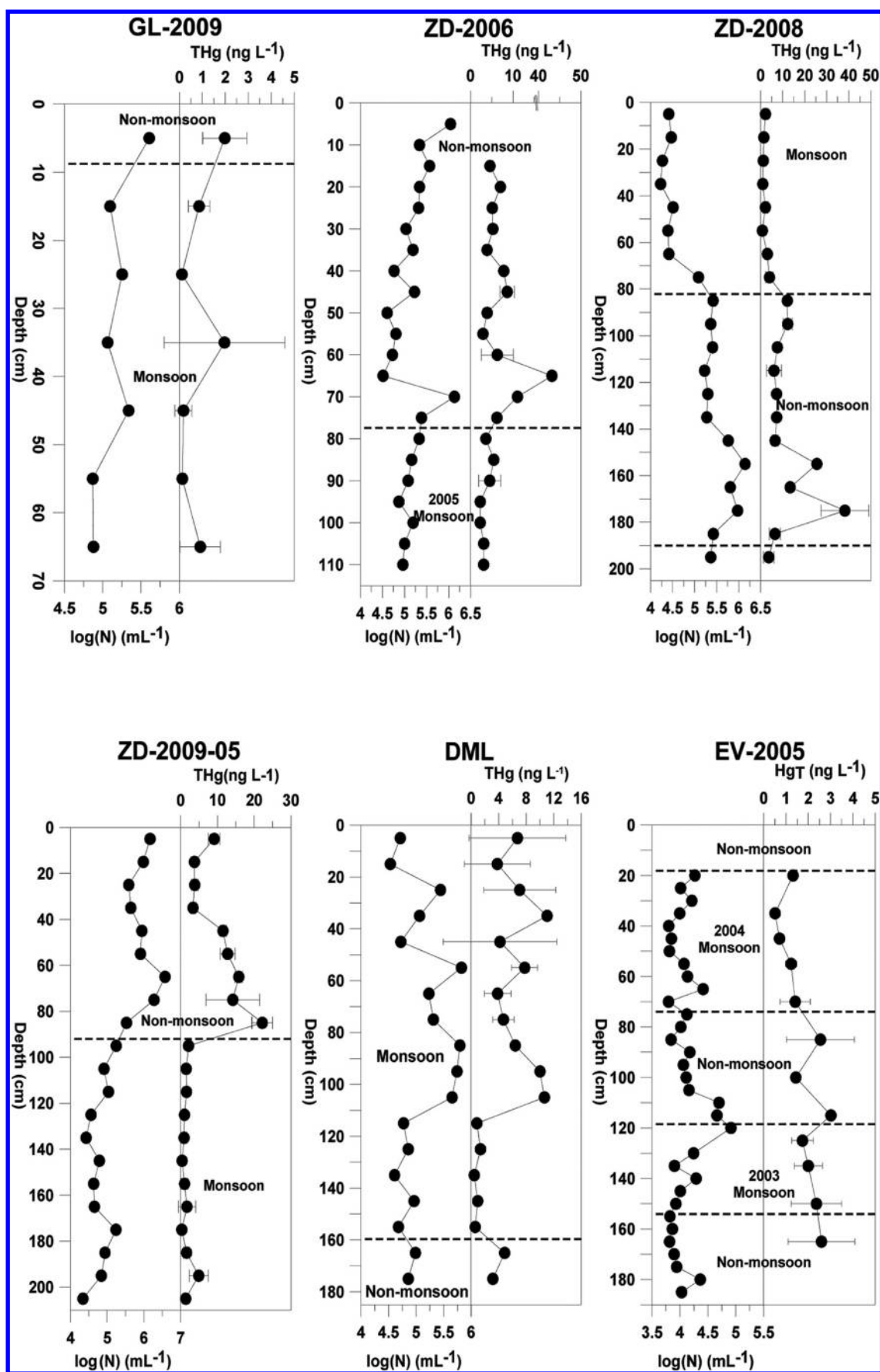


Figure 2. continued

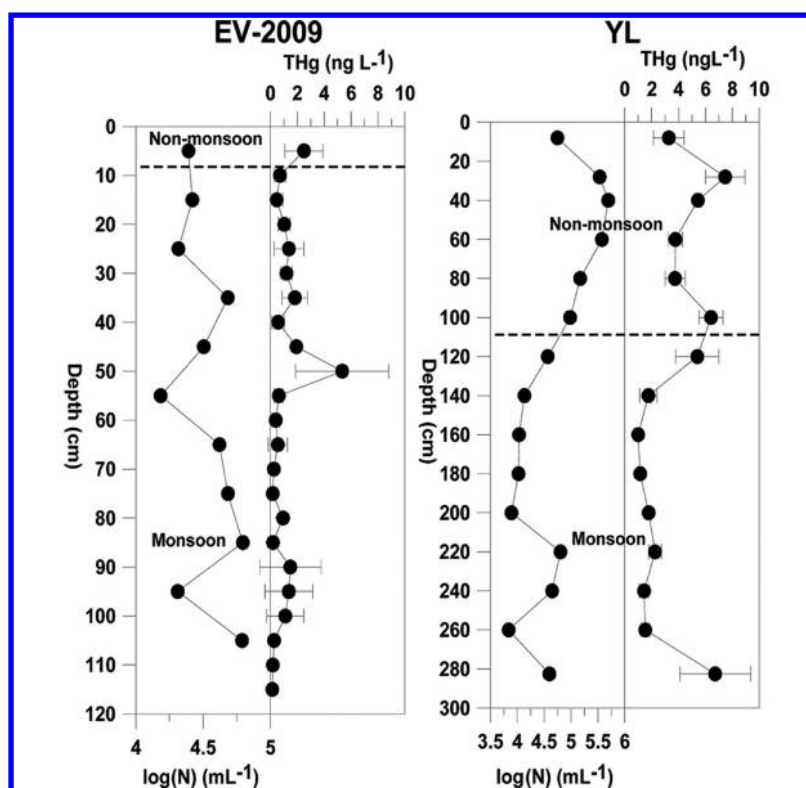


Figure 2. Depth profiles of the concentrations of total mercury (THg) (ng L^{-1}) and insoluble particles (N per mL expressed in logarithmic units) in the glacier snowpits from western China.

of Manitoba or Jena MERCUR in a metal-free Class 100 laminar flow hood placed in a Class 1000 cleanroom laboratory at the Key Laboratory of Tibetan Environment Changes and Land Surface Processes (TEL), Institute of Tibetan Plateau Research, Chinese Academy of Sciences (CAS). For each snow sample, 15–25 mL meltwater was taken for THg detection. The method detection limit for THg in both laboratories was less than 0.2 ng L^{-1} . Field blank samples were collected during each sampling and their THg concentrations were always lower than 0.3 ng L^{-1} . Certified reference materials ORMS-2 and ORMS-3 (National Research Council of Canada) were used for QA/QC, and the recoveries were within 5% of their certified values. To further ensure the data quality, ZD-2008 snowpits were measured in both laboratories and the differences were within 15%.

$\delta^{18}\text{O}$ was quantified at TEL using a MAT-253 isotope ratio mass spectrometer with a precision of $\pm 0.2\%$. Analysis of major cations (Ca^{2+} , Mg^{2+} , Na^{+} , and K^{+}) was carried out on a Dionex ISC 2000 ion chromatograph equipped with a CSES suppresser using an IonPac CS12A column and 20 mM methanesulfonic acid (MSA) as the eluent. Major anions (Cl^{-} , NO_3^{-} , and SO_4^{2-}) were measured on a Dionex ISC 2500 ion chromatograph equipped with an ASRS suppresser using an IonPac AS11-HC column and 25 mM KOH as the eluent. The detection limits were $1 \mu\text{g L}^{-1}$ for all ions and analytical precision was within 5%.

Insoluble particles were measured by a 256-channel Coulter Counter (Multisizer III, Beckman Coulter) in a class 100 clean room at the State Key Laboratory of Cryospheric Sciences, CAS. Prior to analysis, 2.5 mL samples were extracted from the sample containers using a pipette and diluted 1:4 with 2% NaCl. The particle sizes reported here were spherical equivalent diameters ranging from 1.0 to $30 \mu\text{m}$.

Determination of Seasonality of Snow Accumulation.

The seasonality of the snow accumulation on the glaciers was determined based on $\delta^{18}\text{O}$ and major ion profiles in the snow. This is possible because of the dramatic differences in climatology in western China (Supporting Information). In general, $\delta^{18}\text{O}$ values in snow in the southern Tibetan Plateau are more negative in summer than in winter, due to the dominance of the Indian summer monsoon, typically from June to September. In the northern Tibetan Plateau and the Xinjiang Region where the impact of the Indian monsoon is negligible, $\delta^{18}\text{O}$ values are mainly influenced by air temperature, with less negative values in summer than in winter.^{9,10} The seasonality determined based on $\delta^{18}\text{O}$ is further verified with the major ion profiles in snowpits, which are more consistent throughout the entire region, with lower concentrations in summer and higher concentrations in winter, mainly due to enhanced dust aerosol deposition in winter when it is drier.^{11,12} It should be noted that some of the snowpits (e.g., MSD and TS) were subjected to strong melt during summer when the air temperature reached above 0°C . For those snowpits, only annual accumulations were determined.

RESULTS

As shown in Figure 2 and Table S2 of the Supporting Information, THg concentrations in glacier snow over western China varied over a wide range from <1 to 43.6 ng L^{-1} . Three of the sampling sites, GL, ZD, and EV, were revisited in several years. Except the GL site where the 2009 values were lower than those measured in 2005, all of the other repeated measurements agreed with each other very well, indicating that the data reported here are repeatable.

In general, THg concentrations in the glacier snowpits from western China were comparable with those reported for the

central and southern Tibetan Plateau,^{6,7} the Upper Fremont Glacier of USA,¹³ the Summit Station in Greenland,¹⁴ and the Commonwealth Glacier in the Antarctic,¹⁵ and were at the lower end of those reported in the Alps.^{16–18} Higher average THg concentrations were generally found in glacier snowpits in the northern region (e.g., MSD, TS and LH) where THg were typically $>10 \text{ ng L}^{-1}$, while those in the southern region (e.g., EV) were lower, typically $<3 \text{ ng L}^{-1}$ (Table S2 of the Supporting Information).

As expected, the THg concentrations fluctuated with depth in the glacier snowpits (Figure 2), though the variability is highly site specific. In general (Table S3 of the Supporting Information), snowpits from the southern region where the monsoon dominates in summer, average THg concentrations were several times higher in the nonmonsoon season than those in the monsoon season. In contrast, at the LH site located in the northern part of the Tibetan Plateau, which is hardly influenced by the Indian summer monsoon, the THg concentrations did not show significant seasonality. Slightly higher concentrations were observed in summer, mainly due to several peaks associated with the dust layers as reported earlier.⁶ In northwestern China, the seasonality can only be determined at site MS in the southeastern part of the Pamir, where THg showed no clear seasonal trend.

When comparing the profiles of THg with those of other parameters such as particles and major ions in the snowpits (Figure 2 and Figure S2 of the Supporting Information), the THg concentrations covaried most similarly to that of Ca^{2+} and/or particles for most of the snowpits (Table S4 of the Supporting Information). This similarity is most obvious in the ZD and DML sites. There are, however, some clear mismatches. For example, in the ZD-2006 snowpit, the THg concentration was the highest at 65 cm below the snow surface (the 13th sampling layer; 43.2 ng L^{-1}), at the same depth the particle concentration was very low, but peaked in the next sampling layer. For the GL snowpits, particle profiles fluctuated while those of THg did not exactly mirror the trend. For those snowpits that were subjected to melting such as MSD and TS, profiles of THg showed no clear similarity with those of other parameters.

DISCUSSION

Snowpit Hg Records and Atmospheric Hg. Chemical records derived from glacier snow and ice can reflect changes in modern and past atmospheric loadings (e.g., refs 19–21). Given that most of the sampling sites in this study, especially on the Tibetan Plateau, are far away from point sources of anthropogenic Hg emission, snowpit Hg records should reflect the background levels of atmospheric Hg over the study area. The high covariation between Hg and particles further supports our previous findings that particle-bound Hg dominates the snowpit Hg⁶ and that aerosols play an important role in atmospheric Hg transport and deposition over western China. Situated in central Asia, Western China is surrounded by and is itself an arid region (Figure S1 of the Supporting Information). As such, there is notable spatiotemporal variability of dust loading in the free atmosphere, which corresponds to a similar variation in the snowpit THg records. Spatially, the northern region has usually high atmospheric dust loading because it receives less precipitation and is closer to the major dust source regions (e.g., Qaidam Basin and Taklimakan Desert). Seasonal variability varied with regions. For instance, on the Tibetan Plateau, dust storms are a frequent phenomenon in winter and

especially in spring,^{22,23} while in summer, less dust is entrained in the air due to lower wind speeds and enhanced aerosol washout by high precipitation, leading to lower atmospheric Hg deposition. In the northern region, dust storm frequency is relatively decentralized and occurs periodically in summer,²² which can be seen in the THg records of LH and MS with a relatively flat seasonality pattern (Figure S2 of the Supporting Information). The general variations in THg of “higher/lower in north/south” and “higher/lower in winter/summer” in western China are thus attributable to changes in atmospheric particle loadings.

When considering the association between atmospheric deposition of Hg and particles, it should be noticed that Hg, unlike any other metals, exists in ambient air predominantly in the vapor phase¹ as gaseous elemental mercury (GEM or Hg^0). Atmospheric deposition of GEM in snow is likely negligible unless GEM is converted to the other two species of atmospheric Hg, namely reactive gaseous mercury (RGM, $\text{Hg}(\text{II})$) and particulate Hg (PHg). Although constituting typically less than 10% of the atmospheric Hg,¹ RGM, and PHg are more prone to deposition than GEM.²⁴ It is known that PHg, most if not all, is likely retained within snow, whereas the fate of deposited RGM is far more complicated than that of GEM and PHg.³ Furthermore, Hg within snowpack can undergo various postdepositional transformation processes (section below). Therefore, Hg profiles reconstructed from snowpits are not necessarily indicative of total atmospheric Hg deposition; rather, they are more representative of the net retention of atmospheric Hg.

Post-Depositional Processes. Mercury, once deposited into snow and ice packs, is subject to postdepositional processes and is highly labile particularly in exposed snow.^{25,26} Three major postdepositional processes have been proposed: (1) percolation, (2) settling of PHg, and (3) photoreduction of $\text{Hg}(\text{II})$, which may then be emitted back to the atmosphere as GEM.²⁶ Furthermore, sublimation, ablation, and drifting inducing mass loss of snow may also lead to changes in THg concentrations.

Photoreduction occurs significantly at the snow surface, perhaps in the top few centimeters,²⁷ and is limited deeper in the snowpack due to less availability of solar radiation. Field observation suggested that newly deposited Hg in a snow episode decreased by an average of 54% within 24 h after deposition.²⁶ Such photoreduction could be significant at high altitude regions in western China due to enhanced UV radiation. Therefore, Hg concentrations in the uppermost snow layer could reach background concentrations within days or even faster. Settling of aerosols may lead to removal of Hg from the uppermost snow layers, transporting PHg to lower strata. This process would most likely occur during the melting period when particles are moving downward, resulting in increasing Hg concentrations with depth. However, the lack of a persistently increasing trend in THg with depth in most of the snowpit profiles (Figure 2) suggests that settling of aerosols is negligible unless glacier snow melts at a considerable rate.

Despite lack of evidence of a general downward movement of Hg with particles, percolation of water-soluble Hg could episodically occur at low elevation sites when temperature rises above 0°C in summer. This is evident at sites TS and MSD where $\delta^{18}\text{O}$ profiles are rather flat across the depth or where major ice layers were observed (Figure S2 of the Supporting Information). As shown in Figures 2 and Figure S2 of the Supporting Information, despite the high consistency and close

Table 1. Estimated Seasonal and Annual Atmospheric Deposition Fluxes of Mercury Based on Snowpit Records over Western China (Unit: $\mu\text{g m}^{-2} \text{yr}^{-1}$)

site	year	season			annual flux
MSD	2010				3.62
	2009				1.44
TS	2008				3.84
	2007				4.63
LH	2008	fall	summer	spring	3.91
		1.27	1.56	1.08	
MS	2009–2010		summer	spring and winter	1.89
			0.26	1.63	
GL	2005	monsoon	nonmonsoon		0.99
		0.14	0.85		
ZD	2009	0.15			2.97
	2005–2006	0.52	2.45		
	2007–2008	0.66	7.23		
	2008–2009	0.87	3.83		
DML	2008	3.88			4.23
EV	2003–2004	0.31	0.43		0.74
	2008	0.46			
YL	2008–2009	2.11	2.08		4.19

relationships of most ionic profiles, both THg and particles showed unique variation patterns which are different to those of major ions (Table S4 of the Supporting Information), indicating that THg does not move consistently with particles and ions during percolation. For instance, in the TS snowpit, most major ions were depleted and showed rather flat profiles downward of 100 cm, whereas THg and particles showed fluctuations; THg concentration in the depth of 170–180 cm is the highest even though there was a particle enrichment at ~95 cm, possibly because Hg has been percolated through the upper dust layer and moved downward. Site MSD is located at the lowest elevation, where all THg peaks appear in ice layers without a large amount particles (Figure S2 of the Supporting Information). This is further evidence that Hg was depleted during percolation and then reaccumulated during the refreezing of Hg-enriched meltwater. This would not occur if melting proceeds thoroughly as in the spring melting season in the polar regions. Dommergue et al.²⁸ found that during snowmelt in a sub-Arctic site, 90% of Hg is likely released with the meltwater in the snow surface. Many studies have reported that Hg is included in the ionic pulse at the onset of melting.^{29–31} Melting in high-altitude glaciers does not occur all at once but rather, during late spring and summer, glacier snow starts to melt when the ambient surface-level temperature reaches a few degrees below freezing in the daytime.³ Percolation columns form within the snowpack and channel meltwater containing significant Hg downward, which will refreeze when temperature drops. The melting time window depends on the periodic cycle of temperature and after repeated melt–refreeze cycles, an ice layer can be formed and then becomes an effective barrier to infiltration of subsequent percolation in upper layers. Thus, depleted Hg from upper snow layers could accumulate to a significant amount in ice layers, as in MSD and ZD-2008 (Figure S2 of the Supporting Information). Nevertheless, ions and particles do not peak in the ice layers, further suggesting that percolation of Hg is not synchronous with that of particle and ions.

Role of Particles in THg Distribution in Glacier Snow.

The relatively strong relationship between THg and particles in glacier snow over western China implies that THg is likely

predominately preserved in the form of PHg. This is supported by several lines of evidence: 1) PHg is readily scavenged during both wet and dry deposition processes, and once deposited onto snow, PHg is likely far less photoreducible than RGM and is thus strongly retained by glacier snow.³ Previous studies in Antarctic, Arctic, and alpine sites as well as many other regions have also showed that PHg is well associated with dust and particles present in snow (ref³ and literatures therein); 2) Zhang et al.³² suggested that dry depositional fluxes of atmospheric dust contributed more than 90% of the total deposition of dust over the Tibetan Plateau. In general more than 50% of the dust emission and storm events over western China occur in spring,²² which coincides with the seasonality of the profiles of THg and particles. PHg concentrations were further quantified in a shallow snowpit dug at site ZD in 2010. Results showed that PHg constituted up to 97% of the glacier snow Hg with an average of 48% (Figure S3 of the Supporting Information). A strong correlation ($R^2 = 0.98$, $P < 0.01$) was found between THg and PHg, confirming that PHg is a dominant factor in glacier snow Hg distribution.

Inconsistent variation in profiles of THg and particles in some snowpits suggests that the connection between two variables could be lost during postdepositional processes in certain snow layers. Nevertheless, when averaging out values of measured parameters for each snowpit, a significant, positive correlation was found between THg and particles ($R^2 = 0.62$, $P < 0.01$, Figure S4 of the Supporting Information), whereas correlations between THg and ions were not statistically significant. Similar correlation patterns were also found for minimum and maximum values of measured parameters for all sampling snowpits (Table S5 of the Supporting Information). This suggests that, although postdepositional processes could redistribute Hg and other parameters in glacier snow, resulting in inconsistent variation of THg and particles at times, at large geographical scales, particulate matter is the dominant factor influencing the levels and distribution patterns of THg in glacier snow. Therefore, concentrations of particles may serve as a good predictor of THg concentrations in glacier snow over western China and perhaps in other low- to mid-latitude regions of central mountainous Asia.

Atmospheric Hg Depositional Flux Inferred from Snowpit Hg Concentration. Atmospheric Hg is deposited by wet and dry processes. While measurement of wet deposition flux is relatively straightforward, measurement techniques for Hg dry deposition remain to be standardized.³³ Hg dry deposition can contribute amounts of mercury to the land surface as much as or even greater than wet deposition.^{34,35} Given the general lack of precipitation and the dominant role of dry deposition fluxes of atmospheric dust over western China, Hg dry deposition could be substantial when compared with wet deposition. Glaciers, exposed directly to the ambient air, are capable of receiving and preserving both wet and dry atmospheric deposition, therefore are potentially robust in preserving overall deposited atmospheric Hg. Atmospheric Hg depositional fluxes (FHg) over western China were estimated using the snowpit records. FHg for a given site was first calculated for each sampling layer based on corresponding THg concentration and snow density, which was then summed up cumulatively for a given season or year. The estimated annual FHg ranged from 0.74 to 7.89 $\mu\text{g m}^{-2} \text{yr}^{-1}$ (Table 1), which agrees very well with the global natural FHg rate of 2–5 $\mu\text{g m}^{-2} \text{yr}^{-1}$.³⁶ Recent studies based on lake sediment records have estimated the accumulation rates of FHg on the Tibetan Plateau ranged from 5.1 to 7.9 $\mu\text{g m}^{-2} \text{yr}^{-1}$ during recent years,^{37,38} which is near the higher end of the FHg estimated in this study based on the snowpit records. This is not surprising, as lake sediments receive Hg from both atmospheric deposition and riverine discharge within watersheds.³⁶

The close agreement between these records suggest that postdepositional loss of THg in the snowpits at these high altitude glaciers is negligible due to the dominance of less reactive and less mobile PHg in the snowpits in this region. This supports the use of THg records in glacier snowpits as a practical tool for estimating atmospheric Hg depositions in vastly remote and harsh terrains such as western China where long-term monitoring data of atmospheric Hg levels and deposition do not exist.

Despite its close proximity to Eastern China and South Asia, two of the most concentrated anthropogenic Hg emission regions in the world,^{39,40} western China exhibited background atmospheric FHg, which is one to three orders of magnitude lower than that of East Asia.^{41–44} This is possible due to its high elevation topography and upwind geographical location, which is less influenced by anthropogenic Hg emissions from surrounding areas. This should be taken into consideration when modeling or assessing regional or global Hg depositions.

Implications for the Terrestrial and Aquatic Environment in Western China and Beyond. Glaciers act as temporary reservoirs of atmospheric deposited chemicals. Melting glaciers as secondary sources of chemical contaminants (e.g., persistent organic pollutants) has been reported in other remote alpine regions.^{45,46} Upon snowmelt, Hg is depleted from snow and most of it is subsequently released to meltwater-fed catchments (i.e., soil and aquatic systems), potentially yielding a pulse of elevated Hg.^{28,30} Glaciers over western China have been undergoing extensive recession and an estimated 500 km³ (~450 km³ water equivalence) volume of glaciers have been lost in the last 40 years.⁴⁷ Assuming THg concentration in glacier snow is 5.6 ng L⁻¹ (average THg concentrations for all snowpit samples), it can be estimated that 2.5 tonnes of Hg have been released from glaciers to the meltwater-fed lower ecosystem over this period. This is likely

an underestimation because the recession of glaciers is the ultimate balance of dynamic processes during which more meltwater is produced. Taking Lake Nam Co, one of the largest lakes (4725 m a.s.l., 2000 km² surface area) in central Tibet, as an example, it is mainly supplied by precipitation, glacier and snow meltwater, and other sources such as underground water. Glacier meltwater constitutes only 11% of the total water supply but accounts for 50.6% of the positive lake water balance post-1990.⁴⁸ Therefore, glaciers might act as an important Hg supplier to downstream aquatic systems. Glacier retreat is expected to continue and the predicted reduction of glacier volume in China is 1690–3760 km³ in the 21st century⁴⁹ and accordingly Hg loss via glacier melt is estimated to be 8.5–19 tonnes. Thus, the role of glaciers as a source of Hg for aquatic ecosystems will be enhanced in the foreseeable future. If taking seasonal snowpack (generally forms in winter and melts in spring) into consideration, the amount of Hg released by meltwater will increase significantly. This is of particular concern in western China as it is the source water for many large rivers in Asia.

■ ASSOCIATED CONTENT

● Supporting Information

Detailed information about the geographic setting and climatology of the study area, sampling sites, snowpit profiles of all-measured physical and chemical parameters and other supplementary results. This material is available free of charge via the Internet at <http://pubs.acs.org>.

■ AUTHOR INFORMATION

Corresponding Author

*E-mail: Shichang.Kang@itpcas.ac.cn, Tel/Fax: +86-10-84097092.

Notes

The authors declare no competing financial interest.

■ ACKNOWLEDGMENTS

This work was supported by the National Natural Science Foundation of China (40830743 & 41101064), the State Key Laboratory of Cryospheric Sciences (SKLCS-ZZ-2008-01 & SKLCS 09-06), the Natural Science and Engineering Research Council of Canada, and the Special Funds for Dean's Award Winners. The authors are grateful to field staff for their hard and excellent glacier sampling work. Special thanks are owed to Dr. Aurélien Dommergue for his constructive criticism.

■ REFERENCES

- (1) Schroeder, W. H.; Munthe, J. Atmospheric mercury - An overview. *Atmos. Environ.* **1998**, 32 (5), 809–822.
- (2) Steffen, A.; Douglas, T.; Amyot, M.; Ariya, P.; Aspmo, K.; Berg, T.; Bottenheim, J.; Brooks, S.; Cobbett, F.; Dastoor, A.; Dommergue, A.; Ebinghaus, R.; Ferrari, C.; Gardfeldt, K.; Goodsite, M. E.; Lean, D.; Poulain, A. J.; Scherz, C.; Skov, H.; Sommar, J.; Temme, C. A synthesis of atmospheric mercury depletion event chemistry in the atmosphere and snow. *Atmos. Chem. Phys.* **2008**, 8 (6), 1445–1482.
- (3) Durnford, D.; Dastoor, A. The behavior of mercury in the cryosphere: A review of what we know from observations. *J. Geophys. Res.-Atmos.* **2011**, 116, D06305.
- (4) Wu, L. Z.; Li, X., *China Glacier Information System (in Chinese)*; China Ocean Press: Beijing, 2004.
- (5) Huang, X.; Sillanpaa, M.; Duo, B.; Gjessing, E. T. Water quality in the Tibetan Plateau: Metal contents of four selected rivers. *Environ. Pollut.* **2008**, 156 (2), 270–277.

- (6) Loewen, M.; Kang, S.; Armstrong, D.; Zhang, Q.; Tomy, G.; Wang, F. Atmospheric transport of mercury to the Tibetan plateau. *Environ. Sci. Technol.* **2007**, *41* (22), 7632–7638.
- (7) Wang, X. P.; Yao, T. D.; Wang, P. L.; Yang, W.; Tian, L. D. The recent deposition of persistent organic pollutants and mercury to the Dasuopu glacier, Mt. Xixiabangma, central Himalayas. *Sci. Total Environ.* **2008**, *394* (1), 134–143.
- (8) EPA, U. S., *Method 1631, Revision E: Mercury in water by oxidation, purge and trap, and cold vapor atomic fluorescence spectrometry*. United States Environmental Protection Agency: Washington, DC, 2002.
- (9) Dansgaard, W. Stable isotopes in precipitation. *Tellus* **1964**, *16* (4), 436–468.
- (10) Zhang, X. P.; Masoyoshi, N.; Yao, T. D.; Han, J. K.; Xie, Z. C. Variations of stable isotopic compositions in precipitation on the Tibetan Plateau and its adjacent regions. *Sci. China Ser. D – Earth Sci.* **2002**, *45* (6), 481–493.
- (11) Xiao, C.; Kang, S. C.; Qin, D.; Yao, T. D.; Ren, J. W. Transport of atmospheric impurities over the Qinghai-Xizang (Tibetan) Plateau as shown by snow chemistry. *J. Asian Earth Sci.* **2002**, *20* (3), 231–239.
- (12) Kang, S. C.; Mayewski, P. A.; Qin, D. H.; Sneed, S. A.; Ren, J. W.; Zhang, D. Q. Seasonal differences in snow chemistry from the vicinity of Mt. Everest, central Himalayas. *Atmos. Environ.* **2004**, *38* (18), 2819–2829.
- (13) Schuster, P. F.; Krabbenhoft, D. P.; Naftz, D. L.; Cecil, L. D.; Olson, M. L.; Dewild, J. F.; Susong, D. D.; Green, J. R.; Abbott, M. L. Atmospheric mercury deposition during the last 270 years: A glacial ice core record of natural and anthropogenic sources. *Environ. Sci. Technol.* **2002**, *36* (11), 2303–2310.
- (14) Fain, X.; Ferrari, C. P.; Dommergue, A.; Albert, M.; Battle, M.; Arnaud, L.; Barnola, J. M.; Cairns, W.; Barbante, C.; Boutron, C. Mercury in the snow and firn at Summit Station, Central Greenland, and implications for the study of past atmospheric mercury levels. *Atmos. Chem. Phys.* **2008**, *8* (13), 3441–3457.
- (15) Witherow, R. A.; Lyons, W. B. Mercury deposition in a polar desert ecosystem. *Environ. Sci. Technol.* **2008**, *42* (13), 4710–4716.
- (16) Ferrari, C. P.; Dommergue, A.; Veyseyre, A.; Planchon, F.; Boutron, C. F. Mercury speciation in the French seasonal snow cover. *Sci. Total Environ.* **2002**, *287* (1–2), 61–69.
- (17) Fain, X.; Grangeon, S.; Bahlmann, E.; Fritsche, J.; Obrist, D.; Dommergue, A.; Ferrari, C. P.; Cairns, W.; Ebinghaus, R.; Barbante, C.; Cescon, P.; Boutron, C. Diurnal production of gaseous mercury in the alpine snowpack before snowmelt. *J. Geophys. Res. – Atmos.* **2007**, *112*, D21311.
- (18) Maruszczak, N.; Larose, C.; Dommergue, A.; Yumvihoze, E.; Lean, D.; Nedjai, R.; Ferrari, C. Total mercury and methylmercury in high altitude surface snow from the French Alps. *Sci. Total Environ.* **2011**, *409* (19), 3949–3954.
- (19) Thompson, L. G.; Yao, T.; Davis, M. E.; Henderson, K. A.; Mosley-Thompson, E.; Lin, P. N.; Beer, J.; Synal, H. A.; ColeDai, J.; Bolzan, J. F. Tropical climate instability: The last glacial cycle from a Qinghai-Tibetan ice core. *Science* **1997**, *276* (5320), 1821–1825.
- (20) Zhang, Q. G.; Kang, S. C.; Kaspari, S.; Li, C. L.; Qin, D. H.; Mayewski, P. A.; Hou, S. G. Rare earth elements in an ice core from Mt. Everest: Seasonal variations and potential sources. *Atmos. Res.* **2009**, *94* (2), 300–312.
- (21) Yao, T. D.; Wu, G. J.; Pu, J. C.; Jiao, K. Q.; Huang, C. L. Relationship between calcium and atmospheric dust recorded in Guliya ice core. *Chin. Sci. Bull.* **2004**, *49* (7), 706–710.
- (22) Wang, S. G.; Wang, J. Y.; Zhou, Z. J.; Shang, K. Z. Regional characteristics of three kinds of dust storm events in China. *Atmos. Environ.* **2005**, *39* (3), 509–520.
- (23) Wang, X. M.; Dong, Z. B.; Zhang, J. W.; Liu, L. C. Modern dust storms in China: an overview. *J. Arid Environ.* **2004**, *58* (4), 559–574.
- (24) Lin, C. J.; Pongprueksa, P.; Lindberg, S. E.; Pehkonen, S. O.; Byun, D.; Jang, C. Scientific uncertainties in atmospheric mercury models I: Model science evaluation. *Atmos. Environ.* **2006**, *40* (16), 2911–2928.
- (25) Lalonde, J. D.; Amyot, M.; Doyon, M. R.; Auclair, J. C. Photo-induced Hg(II) reduction in snow from the remote and temperate Experimental Lakes Area (Ontario, Canada). *J. Geophys. Res. – Atmos.* **2003**, *108* (D6), 4200–4207.
- (26) Lalonde, J. D.; Poulain, A. J.; Amyot, M. The role of mercury redox reactions in snow on snow-to-air mercury transfer. *Environ. Sci. Technol.* **2002**, *36* (2), 174–178.
- (27) Dommergue, A.; Ferrari, C. P.; Poissant, L.; Gauchard, P. A.; Boutron, C. F. Diurnal cycles of gaseous mercury within the snowpack at Kuujuaupik/Whapmagoostui, Quebec, Canada. *Environ. Sci. Technol.* **2003**, *37* (15), 3289–3297.
- (28) Dommergue, A.; Ferrari, C. P.; Gauchard, P. A.; Boutron, C. F.; Poissant, L.; Pilote, M.; Jitaru, P.; Adams, F. C. The fate of mercury species in a sub-arctic snowpack during snowmelt. *Geophys. Res. Lett.* **2003**, *30* (12), 1621–1624.
- (29) Allan, C. J.; Heyes, A.; Roulet, N. T.; Louis, V. L.; St; Rudd, J. W. M. Spatial and temporal dynamics of mercury in Precambrian Shield upland runoff. *Biogeochemistry* **2001**, *52* (1), 13–40.
- (30) Dommergue, A.; Larose, C.; Fain, X.; Clarisse, O.; Foucher, D.; Hintelmann, H.; Schneider, D.; Ferrari, C. P. Deposition of mercury species in the Ny-Alesund area (79 degrees N) and their transfer during snowmelt. *Environ. Sci. Technol.* **2010**, *44* (3), 901–907.
- (31) Lindberg, S. E.; Brooks, S.; Lin, C. J.; Scott, K. J.; Landis, M. S.; Stevens, R. K.; Goodsite, M.; Richter, A. Dynamic oxidation of gaseous mercury in the Arctic troposphere at polar sunrise. *Environ. Sci. Technol.* **2002**, *36* (6), 1245–1256.
- (32) Zhang, X. Y.; Arimoto, R.; Cao, J. J.; An, Z. S.; Wang, D. Atmospheric dust aerosol over the Tibetan Plateau. *J. Geophys. Res. – Atmos.* **2001**, *106* (D16), 18471–18476.
- (33) Lyman, S. N.; Gustin, M. S.; Prestbo, E. M.; Kilner, P. I.; Edgerton, E.; Hartsell, B. Testing and application of surrogate surfaces for understanding potential gaseous oxidized mercury dry deposition. *Environ. Sci. Technol.* **2009**, *43* (16), 6235–6241.
- (34) Graydon, J. A.; Louis, V. L. S.; Hintelmann, H.; Lindberg, S. E.; Sandilands, K. A.; Rudd, J. W. M.; Kelly, C. A.; Hall, B. D.; Mowat, L. D. Long-term wet and dry deposition of total and methyl mercury in the remote boreal ecoregion of Canada. *Environ. Sci. Technol.* **2008**, *42* (22), 8345–8351.
- (35) Zhang, L. M.; Wright, L. P.; Blanchard, P. A review of current knowledge concerning dry deposition of atmospheric mercury. *Atmos. Environ.* **2009**, *43* (37), 5853–5864.
- (36) Swain, E. B.; Engstrom, D. R.; Brigham, M. E.; Henning, T. A.; Brezonik, P. L. Increasing rates of atmospheric mercury deposition in midcontinental North America. *Science* **1992**, *257* (5071), 784–787.
- (37) Wang, X. P.; Yang, H. D.; Gong, P.; Zhao, X.; Wu, G. J.; Turner, S.; Yao, T. D. One century sedimentary records of polycyclic aromatic hydrocarbons, mercury and trace elements in the Qinghai Lake, Tibetan Plateau. *Environ. Pollut.* **2010**, *158* (10), 3065–3070.
- (38) Yang, H. D.; Battarbee, R. W.; Turner, S. D.; Rose, N. L.; Derwent, R. G.; Wu, G. J.; Yang, R. Q. Historical reconstruction of mercury pollution across the Tibetan plateau using lake sediments. *Environ. Sci. Technol.* **2010**, *44* (8), 2918–2924.
- (39) Jiang, G. B.; Shi, J. B.; Feng, X. B. Mercury pollution in China. *Environ. Sci. Technol.* **2006**, *40* (12), 3672–3678.
- (40) Pirrone, N.; Cinnirella, S.; Feng, X.; Finkelman, R. B.; Friedli, H. R.; Leaner, J.; Mason, R.; Mukherjee, A. B.; Stracher, G. B.; Streets, D. G.; Telmer, K. Global mercury emissions to the atmosphere from anthropogenic and natural sources. *Atmos. Chem. Phys.* **2010**, *10* (13), 5951–5964.
- (41) Pan, L.; Lin, C. J.; Carmichael, G. R.; Streets, D. G.; Tang, Y. H.; Woo, J. H.; Shetty, S. K.; Chu, H. W.; Ho, T. C.; Friedli, H. R.; Feng, X. B. Study of atmospheric mercury budget in East Asia using STEM-Hg modeling system. *Sci. Total Environ.* **2010**, *408* (16), 3277–3291.
- (42) Feng, X. B.; Qiu, G. L. Mercury pollution in Guizhou, Southwestern China - An overview. *Sci. Total Environ.* **2008**, *400* (1–3), 227–237.
- (43) Wang, Z. W.; Zhang, X. S.; Chen, Z. S.; Zhang, Y. Mercury concentrations in size-fractionated airborne particles at urban and

suburban sites in Beijing, China. *Atmos. Environ.* **2006**, *40* (12), 2194–2201.

(44) Tan, H.; He, J. L.; Liang, L.; Lazoff, S.; Sommer, J.; Xiao, Z. F.; Lindqvist, O. Atmospheric mercury deposition in Guizhou, China. *Sci. Total Environ.* **2000**, *259* (1–3), 223–230.

(45) Blais, J. M.; Schindler, D. W.; Muir, D. C. G.; Sharp, M.; Donald, D.; Lafreniere, M.; Braekevelt, E.; Strachan, W. M. J. Melting glaciers: A major source of persistent organochlorines to subalpine Bow Lake in Banff National Park, Canada. *Ambio* **2001**, *30* (7), 410–415.

(46) Schmid, P.; Bogdal, C.; Bluthgen, N.; Anselmetti, F. S.; Zwyssig, A.; Hungerbuhler, K. The missing piece: Sediment records in remote mountain lakes confirm glaciers being secondary sources of persistent organic pollutants. *Environ. Sci. Technol.* **2011**, *45* (1), 203–208.

(47) Yao, T. D.; Wang, Y. Q.; Liu, S. Y.; Pu, J. C.; Shen, Y. P.; Lu, A. X. Recent glacial retreat in High Asia in China and its impact on water resource in Northwest China. *Sci. China Ser. D – Earth Sci.* **2004**, *47* (12), 1065–1075.

(48) Zhu, L. P.; Xie, M. P.; Wu, Y. H. Quantitative analysis of lake area variations and the influence factors from 1971 to 2004 in the Nam Co basin of the Tibetan Plateau. *Chin. Sci. Bull.* **2010**, *55* (13), 1294–1303.

(49) Shi, Y. F.; Liu, S. Y. Estimation on the response of glaciers in China to the global warming in the 21st century. *Chin. Sci. Bull.* **2000**, *45* (7), 668–672.